A New Approach for Enhancing Friction Welding Joint Strength

Naseer Malik Abbas
Middle Technical University, Baghdad, Iraq | Institute of Technology, Baghdad, Iraq
nabbas@mtu.edu.iq (corresponding author)

Safaa M. Hassoni
Middle Technical University, Baghdad, Iraq | Institute of Technology, Baghdad, Iraq
drsafaa1970@mtu.edu.iq

Ghusoon Ridha Mohammed Ali
Middle Technical University, Baghdad, Iraq | Institute of Technology, Baghdad, Iraq
ghusoon_ridha@mtu.edu.iq

Received: 1 June 2024 | Revised: 19 June 2024, 26 June 2024, and 5 July 2024 | Accepted: 15 July 2024

 DOI: https://doi.org/10.48084/etasr.7995

ABSTRACT

The current research provides a new approach for enhancing the mechanical characteristics of friction welding joints for AA 6061 T6. Friction welding depends on the contact surface area between the two parts that need to be welded to generate the frictional heat necessary for the welding process. The frictional area is increased by modifying the contact area from flat circles on both sides of the joint to three different design configurations: a truncated cone, a half sphere, and a cylinder along with their opposite cavity. Mechanical characteristics and microstructural behavior for the new joints are studied. It was elucidated that the conical design configuration is the only one that succeeded through specimen manufacturing, welding, and testing procedures. The results show an improvement in the tensile strength of the truncated cone by 12% compared to the basic flat circle configuration. Bending and Vickers Micro-Hardness (HV) also increased in the joint cross-section by 10% and 7%, respectively. The results are consistent with the microstructure tests where the cone design configuration exhibited a finer grain structure than that of the flat circle. This proves that the generated heat is greater in the new design configuration. Thus, it can be said that the current study provides a promising approach for the improvement of friction welding joint strength.

Keywords-friction welding; plastic deformation; mechanical properties; welding joint; AA 6061 T6

I. INTRODUCTION

Friction Welding (FW) is a solid state joining process, in which, like a few other solid state processes, such as Friction Stir Welding (FSW), Friction Stir Processing (FSP), Linear Friction Welding (LFW), and Friction Extrusion (FE), the processed metal reaches to a temperature below the melting point [1-8]. FW is founded on the direct conversion of mechanical power into thermal energy by friction, which makes the processed metal to reach the plastic deformation state. The workpiece that needs to be joined is held stationary in contact with another rotating workpiece under gradually increasing axial force that provides the required pressure for the welding. When the temperature at the interface of the two surfaces in contact rises as a result of friction and applied pressure, welding takes place by halting rotation and maintaining the applied pressure for a predetermined amount of time [9-12]. Due to its high productivity and ease of use, FW is utilized in a variety of applications and is regarded as a cost-effective method. Additionally, because it does not reach melting temperature, friction welding is not as problematic as other fusion welds [3, 7, 9, 10]. FW depends on the friction between the two surfaces in contact to generate the required heat necessary for the welding process. Several studies focused on welding parameter effects, for similar and dissimilar materials, such as rotational speed, axial force (pressure), and holding time on the resulting weld joint quality and strength. Authors in [10] studied the influence of interaction time in FW on the microstructure and tensile properties of dissimilar metal combinations, consisting of eutectoid forming systems (Fe–Ti, Ti–Cu), insoluble system (Fe–Cu), and soluble systems (Fe–Ni and Cu–Ni). The authors stated that increasing the interaction time decreases strength in eutectoid forming and insoluble systems, and increases it in soluble systems. Authors in [13] investigated FW parameters, such as pressure, friction time, upsetting pressure, and upsetting time for AISI430 stainless steel. They conducted tensile, impact, hardness, and microstructure tests and compared the characteristics to the

base materials. Authors in [14] studied the effect of friction parameters, particularly friction time, in continuous drive FW on thermal and mechanical properties and the microstructure of AA6061. They stated that a short friction time results in strong joints. Also, the peak temperature was reached for 3-4 s of the welding process regardless of the duration of the welding procedure. Authors in [15] developed an empirical relationship to anticipate FW joint strength for AA6082 and AISI304 by inspecting welding parameters, like pressure, forging force, friction time, and forging time. They used Response Surface Methodology (RSM) for optimizing the friction welding process parameters. Authors in [16] compared FW and Friction Stir Welding (FSW) by investigating different parameters affecting the characteristics of the joints, such as rotational speed, welding speed, axial force, tool geometry, and defects. They claimed that FSW is superior in welded joints in terms of an adaptation to recent techniques, process parameter optimization, and the capacity of joining a diversity of dissimilar metals and alloys. Authors in [17] studied joining high-density polyethylene rods by rotary FW. They investigated the effect of nanoparticle reinforcement and weld surface shape on the joint strength. Surface shapes used were flat, step, and conic, while ZnO and SiO_2 nanoparticles were used. They found that shape and nanoparticle presence affected the bending strength of the joint and that the step shape had the higher bending strength.

From the literature review and as far as is known, the impact of the interface contact area on the weld joint strength—which is solely responsible for producing the heat needed for the weld—has not been specifically discussed and studied. Thus, the current study presents a new approach for the enhancement of weld joint strength by increasing the interface contact area. The design of the weld joint is modified from a flat circular surface on both sides of the workpieces to three different configurations with their cavities: truncated cone, half sphere, and cylinder.

II. METHODOLOGY

As mentioned above, three distinct configurations were deigned. The design started with the standard tension test specimen according to ASTM E8/E8M – 13a [18], as illustrated in Figure 1(a). Each specimen was cut to two parts. The first part was carved with one side of the design configurations and the other part was carved with its opposite cavity, as evidenced in Figure 1. By doing that, no further machining was required after the welding process. Figure 2 shows a standard tension test specimen. The same procedure was used for the tension test specimens. Standard bending test specimen is according to ASTM E190, as observed in Figure 3.

III. MATHEMATICAL MODELING

The formulas used for calculating the surface area of the designed configurations on the tip of each specimen (Figure 1) are displayed below [19, 20].

- Area of a circle, which is the base for comparing other design configurations:

$$A = \pi R^2 \quad (1)$$

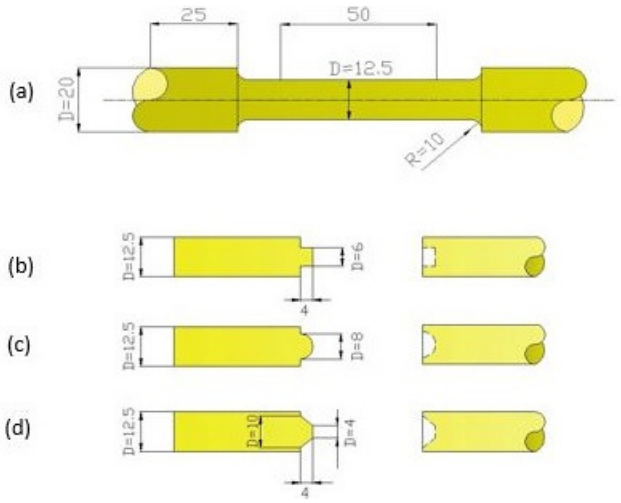

Fig. 1. (a) Standard tension test specimen, (b) cylinder, (c) half sphere, (d) truncated cone.

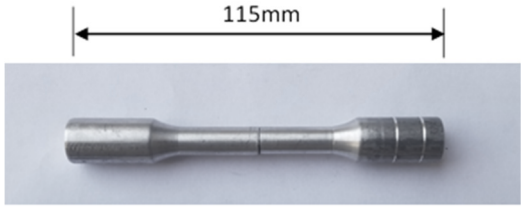

Fig. 2. Standard tension test specimen before welding.

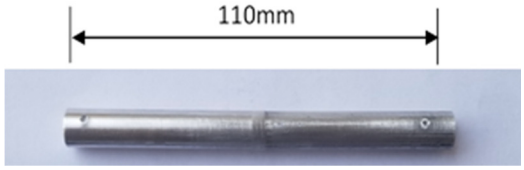

Fig. 3. Standard bending test specimen after welding.

- Total surface area of a cylinder:

$$A_{total} = A_1 + A_2 + A_3 \quad (2)$$

$$A_1 = 2\,\pi\, r\, h \quad (3)$$

$$A_2 = \pi R^2 - \pi r^2 \quad (4)$$

$$A_3 = \pi r^2 \quad (5)$$

where A_1 is the surface area of the cylinder, h is the height of the cylinder, A_2 is the surface area of the ring at the base of the cylinder, and A_3 is the surface area of the circle on the top of the cylinder.

- Total surface area of a half sphere:

$$A_{total} = A_4 + A_5 \quad (6)$$

$$A_4 = \frac{1}{2}(4\,\pi\, r^2) \quad (7)$$

$$A_5 = \pi R^2 - \pi r^2 \quad (8)$$

where A_4 is the surface area of the half sphere and A_5 is the surface area of the ring at the base of the sphere.

- Total surface area of a truncated cone:

$$A_{total} = A_6 + A_7 + A_8 \quad (9)$$

$$A_6 = \pi L\left(R_{large} + r_{small}\right) \quad (10)$$

$$A_7 = \pi R^2 - \pi R_{large}^2 \quad (11)$$

$$A_8 = \pi r_{small}^2 \quad (12)$$

where A_6 is the surface area of the cone, L is the length of the cone's hypotenuse, A_7 is the surface area of the ring at the base of the cone, and A_8: is the surface area of the circle on the top of the cone.

Using the above equations, Table I portrays the percentage increase in the surface area between the base area and the new designed configurations.

TABLE I. SURFACE AREA INCREASE PERCENTAGE

No.	Configuration	Area increase %
1	Circle	Base
2	Cone	35.84 %
3	Half sphere	122.88%
4	Cylinder	61.44%

IV. EXPERIMENTAL PROCEDURES

To ensure repeatability in the tests results, three pairs of each configuration design were made to a total of 24 pairs. The material used is AA 6061 T6 (Al- 1.0Mg - 0.6Si - 0.6Fe - 0.25Cr - 0.2Cu) shaft, which is a widely deployed material in many engineering applications due to its light weight, high strength, and corrosion resistance. The FW machine utilized in this research is a lathe designed and modified to be a FW machine. The machine is equipped with RPM, feed rate, axial force, pressure controllers, and a data acquisition system. Before each welding process, the machine was calibrated and returned to the zero position. Welding data were stored in a text file and were transferred to an Excel file for subsequent processing.

V. RESULTS

Tension test, three points bending test, MH test, and microstructure test were conducted for each specimen of the three configurations and also for the flat base configuration after FW. The FW parameters (rotational speed, axial force, pressure, and holding time after welding) were fixed for all specimens. A study on the optimum parameters was carried out using values from the literature as a starting point, and then applying them to the flat samples to ensure a good weld quality. These parameters were employed afterwards for the other configurations. It should be mentioned that both cylinder and half sphere configurations failed during the welding process, and therefore were not included in the results. The cylindrical design undergoes a stress concentration at its base, and due to the high vibrations of the welding process, the cylinder broke inside its cavity. Regarding the half sphere design, even though the surface area of a half sphere is much larger than the one in the base sample (Table I), the manufacturing of a sphere and its exact cavity is a difficult task. This makes the contact surface areas between the sphere and its cavity to not be exactly the same, leading to weld failure. The truncated cone design configuration eliminates previous problems where the interlock and contact surface areas are more robust. Nevertheless, the manufacturing process for the cone and its cavity should be done accurately and precisely, otherwise it would lead to a weld failure as well. The truncated cone design configuration provides an improved weld joint strength.

A. Tension Tests

A computerized Instron 3369 electromechanical testing machine was used for the tension tests. A standard tension test specimen based on ASTM E8/E8M – 13a was utilized. The tests were conducted at 25 ℃ with a crosshead speed of 0.5mm/min. Figure 4 shows the stress – strain curves for the flat circle and the truncated cone design configurations, while Figure 5 exhibits the flat and truncated cone specimens after the tension test.

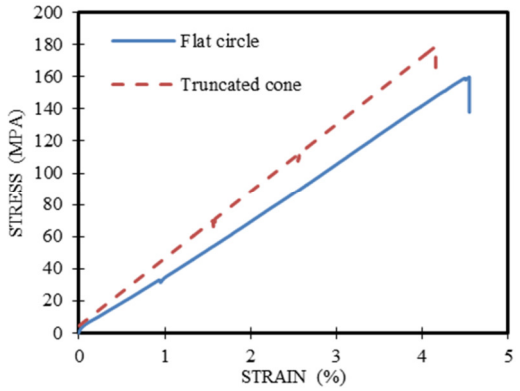

Fig. 4. Stress – strain curves for the flat circle and truncated cone design configurations.

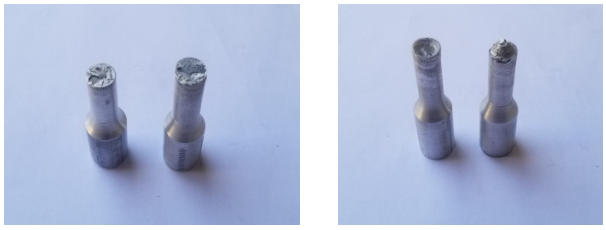

(a) (b)

Fig. 5. (a) Flat and (b) truncated cone specimens after the tension test.

Fig. 6. Three point bending test.

B. Hardness Tests

Vickers MH tests were conducted using a LARYEE digital micro-hardness tester. The average of three readings was taken for the weld joint area for each specimen at a load of 0.98 N. The test results are provided in Table II.

TABLE II. AVERAGE VICKERS MH TESTS RESUJLTS

	Base metal	**Flat circle**	**Truncated cone**
Average Vickers hardness	105	126	135

C. Microstructure Tests

Samples of 10×10 mm from each welded specimen were cut perpendicular to the weld joint and at the centerline of the specimen. Water cooling was used with the cutter and grinder in order to keep the microstructure unchanged. After sample preparation, polishing, and etching, an optical microscope equipped with a camera connected to a computer was employed to perform microstructure studies. The obtained pictures are depicted in Figure 7.

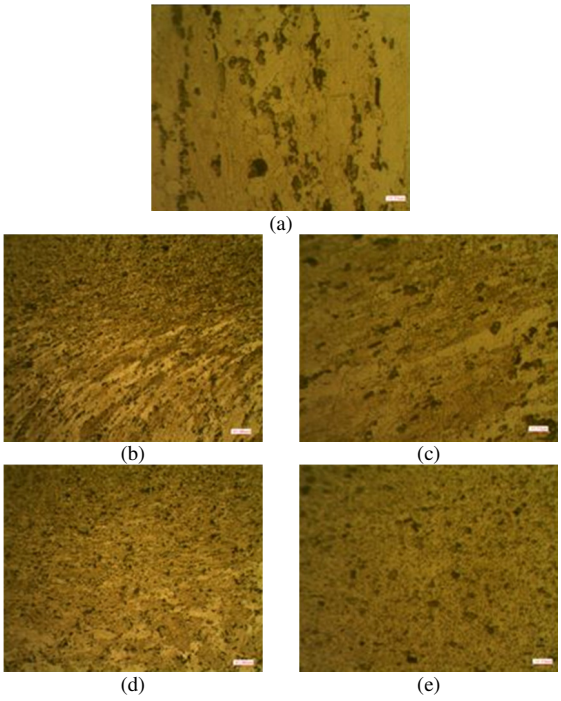

Fig. 7. Microstructure results: (a) Base metal – 10x. (b) Flat circle joint – 10x. (c) Flat circle joint – 40x. (d) Truncated cone design joint – 10x. (e) Truncated cone design joint – 40x.

VI. DISCUSSION

As mentioned above, cylinder and half sphere design configurations failed during the welding process. On the other hand, the truncated cone design configuration provided an excellent interlock between the two parts, in addition to a robust full contact surface area which leads to a perfect weld joint.

The starting point of the discussion will be the microstructure tests observed in Figure 7. The base metal microstructure demonstrated in Figure 7(a) contains large precipitates of the main component elements Al-Mg-Si of this alloy. At the weld joint area of the flat circle and truncated cone design configuration in Figure 7(b), (d), it is very clear that the precipitates are much smaller than in the base metal due to the generated frictional heat, which led to recrystallization. Moreover, the rotation direction of the precipitates during welding is very obvious especially for the flat circle sample. However, the same microstructure at a larger magnification (40x) for a truncated cone (Figure 7(e)) seems finer than for the flat circle (Figure 7(c)). This proves that the heat generated on the truncated cone is more than the heat generated on the flat circle due to the larger contact surface area of the truncated cone.

The stress-strain curves, presented in Figure 4, clearly exhibit that there is an average increase in the tension strength for the truncated cone over the flat circle of about 12 %, and a relative decrease in the total strain rate. Furthermore, both curves display a few points where the stress decreases and rises again, which are caused by the breaks in the weakest points in the structure before the failure during the tension test.

Three point bending tests also demonstrated an increase in the bending strength of about 10 % for the truncated cone over the flat circle. The bending strength for the flat circle joint is 12.4 MPa, while for the truncated cone it is 13.7 MPa. This is due to the truncated cone design, which provides a great interlock between the two welded parts.

Finally, the results of the Vickers MH test for the truncated cone joint are larger than for the flat circle joint. The results revealed an average increase of about 7% (Table II). Tension and MH results are in accordance with the microstructure tests, where a finer grain structure resulted from increased heat input and plastic deformation in cone rather than in circle joint design configuration. The above results are in agreement with what other researchers found when studying the effect of heat on the resulting weld joint for AA 6061 [21-24].

VII. CONCLUSIONS

The current study presented a new approach for improving friction welding joint strength by increasing the contact surface area between the two parts that need to be welded, which has not been studied in the literature. This practice increases the generated frictional heat necessary for welding. Three design configurations were considered for this purpose: a truncated cone, a cylinder, and a half sphere along with their opposite cavities. The conventional flat circle design was considered as the base for comparison with the other design configurations.

Both cylinder and half sphere designs failed during the welding process. The cylindrical design undergoes a stress concentration at the base of the cylinder, and due to the high vibrations of welding process, the cylinder broke inside its cavity. The manufacturing process for a half sphere design and its exact cavity is a difficult task. This makes the contact surface areas between the sphere and its cavity to not exactly match, which led to weld failure. The truncated cone design configuration eliminates such previous problems since the interlock and contact surface areas are more robust.

The tension strength of the truncated cone joint was increased by an average of 12% over the flat circle. Bending strength and Vickers micro-hardness were also increased by 12% and 7%, respectively. A finer grain structure resulted from increased heat input and plastic deformation in truncated cone design configuration.

ACKNOWLEDGMENT

The authors would like to thank the Middle Technical University for making its labs available. Also, many thanks go to Dr. Mustafa K. Ismail and Mr. Ayad K. Abbas for their help in this research.

REFERENCES

[1] A. Vairis and M. Frost, "Modelling the linear friction welding of titanium blocks," *Materials Science and Engineering: A*, vol. 292, no. 1, pp. 8–17, Nov. 2000, https://doi.org/10.1016/S0921-5093(00)01036-4.

[2] M. B. Uday, M. N. Ahmad Fauzi, H. Zuhailawati, and A. B. Ismail, "Advances in friction welding process: A review," *Science and Technology of Welding and Joining*, vol. 15, no. 7, pp. 534–558, Oct. 2010, https://doi.org/10.1179/136217110X12785889550064.

[3] E. D. Nicholas and W. M. Thomas, "A review of friction processes for aerospace applications," *International Journal of Materials and Product Technology*, vol. 13, no. 1–2, pp. 45–55, Jan. 1998, https://doi.org/10.1504/IJMPT.1998.036227.

[4] M. I. Ismail, "The Effect of Shoot Peening on Bending Strength for MIG Weld Joint Aluminum Alloys 2024 T351," *Journal of Techniques*, vol. 30, no. 1, pp. 60–78, 2017.

[5] N. Abbas, X. Deng, X. Li, and A. P. Reynolds, "The compaction and consolidation of machining chips: Experiments and modeling," in *International SAMPE Technical Conference*, Seattle, WA, USA, Dec. 2017, pp. 1096–1109.

[6] N. Abbas, X. Deng, X. Li, and A. Reynolds, "Modeling of heat transfer in compacted machining chips during friction consolidation process," *AIP Conference Proceedings*, vol. 1957, no. 1, Apr. 2018, Art. no. 050005, https://doi.org/10.1063/1.5034335.

[7] A. W. El-Morsy, M. Ghanem, and H. Bahaitham, "Effect of Friction Stir Welding Parameters on the Microstructure and Mechanical Properties of AA2024-T4 Aluminum Alloy," *Engineering, Technology & Applied Science Research*, vol. 8, no. 1, pp. 2493–2498, Feb. 2018, https://doi.org/10.48084/etasr.1704.

[8] N. M. Abbas, X. Deng, and A. P. Reynolds, "Compaction of machining chips: Extended experiments and modeling," *Mechanics of Materials*, vol. 141, Jan. 2020, Art. no. 103249, https://doi.org/10.1016/j.mechmat.2019.103249.

[9] B. S. Yilbas, A. Z. Sahin, N. Kahraman, and A. Z. Al-Garni, "Friction welding of St Al and Al Cu materials," *Journal of Materials Processing Technology*, vol. 49, no. 3, pp. 431–443, Feb. 1995, https://doi.org/10.1016/0924-0136(94)01349-6.

[10] S. D. Meshram, T. Mohandas, and G. M. Reddy, "Friction welding of dissimilar pure metals," *Journal of Materials Processing Technology*, vol. 184, no. 1, pp. 330–337, Apr. 2007, https://doi.org/10.1016/j.jmatprotec.2006.11.123.

[11] N. S. Kalsi and V. S. Sharma, "A statistical analysis of rotary friction welding of steel with varying carbon in workpieces," *The International Journal of Advanced Manufacturing Technology*, vol. 57, no. 9, pp. 957–967, Dec. 2011, https://doi.org/10.1007/s00170-011-3361-z.

[12] N. Shete and S. U. Deokar, "A Review Paper on Rotary Friction Welding," in *International Conference on Ideas, Impact and Innovation in Mechanical Engineering*, Pune, India, Jun. 2017, vol. 5, pp. 1557–1560.

[13] P. Sathiya, S. Aravindan, and A. Noorul Haq, "Effect of friction welding parameters on mechanical and metallurgical properties of ferritic stainless steel," *The International Journal of Advanced Manufacturing Technology*, vol. 31, no. 11, pp. 1076–1082, Feb. 2007, https://doi.org/10.1007/s00170-005-0285-5.

[14] M. A. Tashkandi and M. I. Mohamed, "Effect of Friction Time on the Mechanical and Microstructural Properties of AA6061 Joints by Continuous Drive Friction Welding," *Engineering, Technology & Applied Science Research*, vol. 10, no. 3, pp. 5596–5602, Jun. 2020, https://doi.org/10.48084/etasr.3438.

[15] R. Paventhan, P. R. Lakshminarayanan, and V. Balasubramanian, "Prediction and optimization of friction welding parameters for joining aluminium alloy and stainless steel," *Transactions of Nonferrous Metals Society of China*, vol. 21, no. 7, pp. 1480–1485, Jul. 2011, https://doi.org/10.1016/S1003-6326(11)60884-4.

[16] D. Kumar Rajak, D. D. Pagar, P. L. Menezes, and A. Eyvazian, "Friction-based welding processes: friction welding and friction stir welding," *Journal of Adhesion Science and Technology*, vol. 34, no. 24, pp. 2613–2637, Dec. 2020, https://doi.org/10.1080/01694243.2020.1780716.

[17] V. Asghari, A. Kami, and A. Bagheri, "An investigation on the effect of nanoparticle reinforcement and weld surface shape on bending behavior of rotary friction-welded high-density polyethylene," *Proceedings of the Institution of Mechanical Engineers, Part L: Journal of Materials: Design and Applications*, vol. 236, no. 1, pp. 222–234, Jan. 2022, https://doi.org/10.1177/14644207211044126.

[18] *ASTM E8/E8M-13a(2013), Standard Test Methods For Tension Testing Of Metallic Materials. West Conshohocken, PA, USA: ASTM International, 2013.*

[19] E. Kreyszig, *Advanced Engineering Mathematics*, 10th edition. New York, NY, USA: Wiley, 2010.

[20] "Wolfram MathWorld: The Web's Most Extensive Mathematics Resource." https://mathworld.wolfram.com/.

[21] H. M. Abdul-Aziz, N. M. Abbas, and A. H. Jasim, "Artifitial Aging Time Effect on Corrosion Resistance for Friction Stir Welded AA6061 T6," *Diyala Journal of Engineering Sciences*, vol. 6, no. 3, pp. 83–96, 2013.

[22] S. A. Hussein, A. S. M. Tahir, and M. A. Al-Obaidi, "Evaluation the effects of welding parameters on tri-dissimilar friction stir welds aluminum/steel," *Welding in the World*, vol. 66, no. 11, pp. 2315–2332, Nov. 2022, https://doi.org/10.1007/s40194-022-01360-y.

[23] W. Liu *et al.*, "The Effects of Heat Treatment on Microstructure and Mechanical Properties of Selective Laser Melting 6061 Aluminum Alloy," *Micromachines*, vol. 13, no. 7, Jul. 2022, Art. no. 1059, https://doi.org/10.3390/mi13071059.

[24] S. Prathap Singh, D. X. Tittu George, A. Anitto Joe Xavier, and G. Abinicks Raja, "Effect of heat treatment on the hardness behaviour of the aluminium 6061 alloy," *Materials Today: Proceedings*, Mar. 2023, https://doi.org/10.1016/j.matpr.2023.02.345.